Article

JAC4 Enhances Radiotherapy Effect of NSCLC and Reduces Normal Lung Injury Through Differential Regulation of JWA-Mediated DNA Repair

Luman Wang [1,2,3], Jie Ni [1,2,3], Kun Ding [1,2,3], Chao Zhang [1,2,3], Aiping Li and Jianwei Zhou [1,2,3,*]

[1]Department of Molecular Cell Biology & Toxicology, Center for Global Health, School of Public Health, Nanjing Medical University. 101 Longmian Avenue, Nanjing 211166, China; hdlxdlwlm@126.com (L.W.); 15895572783@163.com (J.N.); dinkun1995@163.com (K.D.); chaozhang2023@163.com (C.Z.); liaiping@njmu.edu.cn (A.L.)
[2]The Key Laboratory of Modern Toxicology, Ministry of Education, School of Public Health, Nanjing Medical University, 101 Longmian Avenue, Nanjing 211166, China
[3]Jiangsu Key Lab of Cancer Biomarkers, Prevention and Treatment, Collaborative Innovation Center for Cancer Medicine, Nanjing Medical University, Nanjing 211166, China.
* Correspondence: jwzhou@njmu.edu.cn; Phone: +86 25 86868421

Abstract: More than 50% of patients with non-small cell lung cancer (NSCLC) are treated with radiotherapy (RT) during different phases of treatment. However, radiation pneumonitis (RP) and resistance often lead to RT failure in NSCLC patients. JWA, a tumor suppressor gene, is known to enhance DNA damage in gastric cancer cells while protect normal cells from DNA damage induced by cisplatin. Recently, we have reported that JWA agonist compound 4 (JAC4) effectively protects intestinal epithelium from RT triggered damage in mice. However, the potential synergistic and attenuated effects of JAC4 in chest RT of lung cancer are not been illuminated. The aim of this study was to investigate the effects of JAC4 on the radiotoxicities of both NSCLC and normal lung tissue. CCK-8 and colony formation assays showed that JAC4 played a bidirectional role in radiation-treated SPCA-1 and BEAS-2B cells. Western blotting and immunofluorescence assays showed that JAC4 in combination with RT increased DNA damage and apoptosis in SPCA-1 cells, while the opposite effect was observed in BEAS-2B cells. Mechanistically, JAC4 inhibited homologous recombination repair (HR) and non-homologous end joining (NHEJ) in SPCA-1 cells, but not in normal cells. JAC4 increased antioxidant capacity, and reduced oxidative stress and inhibited nuclear factor Kappa-B (NF-κB, P65) translocation to the nucleus in BEAS-2B cells. Importantly, the bidirectional roles of JAC4 on RT were reversed by siJWA in both SPCA-1 and BEAS-2B cells. Finally, the bidirectional effects of JAC4 in combination with RT were further validated in NSCLC xenograft model mice. In conclusion, JAC4 enhanced effect of RT on tumor growth while alleviated RP and lung injury. Our results may provide new strategy for optimizing RT regimen for NSCLC.

Keywords: NSCLC; JAC4; radiotherapy; enhanced efficacy and attenuated toxicity; DNA damage repair; oxidative stress

1. Introduction

Lung cancer is the second most common cancer in the world and the leading cause of cancer death worldwide [1]. NSCLC is the most common type of lung cancer, accounting for 80% of all diagnosed lung cancer cases [2, 3]. The treatment of NSCLC mainly includes radiotherapy (RT) and chemotherapy, surgical resection and immunotherapy. Nevertheless, for most patients, NSCLC remains an incurable disease [4]. More than 50% of NSCLC patients receive RT during treatment [5]. However, due to the radiation resistance of tumor tissue and radiation pneumonitis (RP) caused by RT on normal lung

Preprints (www.preprints.org) | NOT PEER-REVIEWED | Posted: 5 June 2023 doi:10.20944/preprints202306.0356.v1

tissue adjacent to cancer, RT failure affects the quality of life of patients [6, 7]. Therefore, the development of radiosensitizers that can effectively increase the toxicity of radiation to cancer tissues while reducing the damage to normal lung tissues will help to improve the clinical treatment effect of NSCLC.

The anti-cancer effect of RT is due by increasing DNA double-strand breaks (DSBs) of cancer cells [8]. HR and NHEJ are main responsible pathways for DNA repair. The key repair proteins of HR and NHEJ include ATR, CHK1, DNA-PKcs, Ku70/Ku80, etc [9]. The dysregulation of DSB repair leads to RT resistance [10]. Therefore, targeted inhibition of these RT related DNA repair molecules can help to increase the radiosensitivity. In addition, the characteristics of high-energy radiation lead to the ionization of water molecules (H_2O) in the lung tissue to produce a large amount of reactive oxygen species (ROS), and triggering oxidative stress and the aggregation of inflammatory cells [11]. NF-κB is a mediator that promotes the induction of inflammatory genes, and its expression is increased after irradiation. Therefore, targeted inhibition of NF-κB can also be used as a radioprotective agent to reduce the inflammatory response in normal lung tissues induced by RT [12, 13].

JWA gene, also known as arl6ip5, is originally cloned from retinoic acid (RA) -induced differentiation model in human bronchial epithelial (HBE) cells. JWA is an environmental response and tumor suppressor gene [14, 15]. The low expression of JWA gene is associated with the poor prognosis of gastric cancer patients; and high expression of JWA inhibits the proliferation, invasion and migration of breast cancer, pancreatic cancer, esophageal squamous cell carcinoma, NSCLC and other cancers [16-20]. Moreover, activation of JWA reverses cisplatin resistance in gastric cancer and trastuzumab-resistant breast cancer [21, 22]. In addition, activation of JWA can inhibit oxidative stress and improve intestinal epithelial homeostasis in radiation enteritis and antagonize paraquat-induced neurotoxicity [23, 24]. JWA plays a bidirectional regulatory role in DNA damage of cancer cells and normal cells caused by chemotherapy [25].

Recent studies have shown that the mimic functional peptide of JWA protein can increase the toxicity of cisplatin on drug-resistant gastric cancer cells while reduce its toxicity on normal cells [25]. JAC4, a specific agonist of JWA gene, can protect the intestine epithelial cells from radiation-induced enteritis through antioxidant/inflammatory signaling [26]. However, it is unknown if JAC4 could exert synergistic and attenuated effects of RT on NSCLC. Herein, we investigated the role of JAC4 and the potential mechanism in NSCLC RT. We found that JAC4 in combination with RT increased DSBs, cell apoptosis and inhibited xenograft tumor growth by blocking DNA repair in NSCLC cells; at the same time, JAC4 protected normal bronchial epithelial cells from RT-induced ROS, DSBs, and inhibited NF-κB-mediated inflammatory response. The bidirectional role of JAC4 was further verified in JWA knockdown cells and validated in NSCLC xenograft RT model mice.

2. Materials and Methods

2.1. Compounds and reagents

JAC4 ($C_{16}H_{13}N_3O_3S$, MW: 327.4) with purity over 98% was synthesized in our laboratory. In this study, polyethylene glycol (40%), ethanol (7.5%), 0.9% normal saline (52.5%) were used to prepare the solution for JAC4. Nuclear and cytoplasmic protein separation kit (P0027); total SOD activity assay kit (S0101S), malondialdehyde (MDA) assay kit (S0131S), catalase assay kit (S0051), and PMSF (100 mM) (ST506) were purchased from Beyotime Biotechnology Co., LTD. (Shanghai, China). Cell/Tissue Total RNA Rapid Extraction Kit (RC112-01), HiScript III RT SuperMix for qPCR (+gDNA wiper) (R323-01), AceQ qRT-PCR SYBR Green Master Mix (Without ROX) (Q121-02) were purchased from Vazyme Biotechnology Co., LTD. (Nanjing, China).

2.2. Cell culture, X-ray irradiation and transfection

Preprints (www.preprints.org) | NOT PEER-REVIEWED | Posted: 5 June 2023 doi:10.20944/preprints202306.0356.v1

Human lung adenocarcinoma cells (SPCA-1) and human bronchial epithelial cells (BEAS-2B) were purchased from Shanghai Institute of Cell Biology, Chinese Academy of Sciences, and cultured in DMEM medium containing 10% fetal bovine serum and 100 g/mL ciprofloxacin in an incubator at 37°C and 5% CO_2. The cells were fully attached to the wall and returned to normal morphology, pretreated with JAC4 (10 μM) for 24 h, and exposed to X-ray irradiation (4 Gy) at a dose rate of 1.25 Gy/min. Cell biology experiments were performed 2 h or 24 h later. For cell transfection, small interfering RNA (siRNA) for JWA (siJWA: 5'- UAAUAGAGCAGGUUGCUCACUACGC -3', Generay, Shanghai, China) and its nonspecific control were synthesized. Both SPCA-1 and BEAS-2B cells were seeded into six-well plates. According to the Lipo 8000™ transfection reagent (Beyotime, Nanjing, China), when the cell density reached 70%, Opti-MEM® Medium 125 μL/well and siJWA (or sicontrol): Lipo 8000TM =100 pmol: 4 μL =25: 1 was mixed then cocultured with cells.

2.3. Cytotoxicity assay

In total of 5,000 SPCA-1 and BEAS-2B cells were inoculated on 96-well plates for 24 h, and irradiated with 0, 4, 8, 12, 16 and 20 Gy, or treated with JAC4 of 0, 1, 5, 10, 20 and 50 μM for 24 h, respectively. CCK-8 reagent was added to each well and incubated in cell incubator for 1 h. Absorbance (OD) was measured at 450 nm. Cell viability calculation formula: cell viability (%) = (OD control group-OD treatment group) ×100% / (OD control group-OD blank hole).

2.4. Western blotting assay

The cell samples were prepared from lysates containing protease and phosphatase inhibitors; animal tumor tissues and lung tissues were fully ground in a mortar with liquid nitrogen, and appropriate amount of lysate containing PMSF and protease phosphatase inhibitor was added, which was fully cracked in a refrigerator at 4°C and centrifuged for use. The protein immunoblotting experiments were carried out according to the protocol [27]. The antibodies used in this study are as follows: anti-JWA (1:100, AbMax, Beijing, China), anti-GAPDH (1:1000, Beyotime, Shanghai, China), anti-Tubulin (1:1000, Beyotime, Shanghai, China), anti-p-p65 (1:1000, Cell Signaling Technology, USA), anti-P65 (1:1000, Santa Cruz, CA, USA), anti-γ-H2AX (1:1000, Servicebio, Wuhan, China), anti-DNA-PKcs (1:1000, Abcam), anti-Ku70 (1:3000, Affinity), anti-p-ATR (1:1000, Cell Signaling Technology, USA), anti-p-CHK1 (1:1000, Cell Signaling Technology, USA).

2.5. Quantitative reverse transcription and polymerase chain reaction (qRT-PCR)

Total RNA was extracted with the Cell/Tissue Total RNA Rapid Extraction Kit, the RNA concentration was determined, and 1 μg total RNA was synthesized into cDNA. AceQ qPCR SYBR Green Master Mix (Vazyme, Nanjing, China) was used in ABI 7900HT real-time PCR system (Applied Biosystems, Carlsbad, CA, USA) for PCR reaction procedure. The primer sequences were indicated as follows:

GAPDH: Forward: 5'- CATCACTGCCACCCAGAAGACTG -3'; Reverse: 5'- ATGCCAGTGAGCTTCCCGTTCAG -3'; IL-10: Forward: 5'- CGGGAAGACAATAACTG-CACCC -3'; Reverse: 5'- CGGTTAGCAGTATGTTGTCCAGC -3'; TNF-α: Forward: 5'- GGTGCCTATGTCTCAGCCTCTT -3'; Reverse: 5'- GCCATAGAACTGATGAGAGGGAG -3'; IL-1β: Forward: 5'- TGGACCTTCCAGGATGAGGACA -3'; Reverse: 5'- GTTCATCTCGGAGCCTGTAGTG -3'; TGF-β1: Forward: 5'- TGATACGCCTGAG-TGGCTGTCT -3'; Reverse: 5'- CACAAGAGCAGTGAGCGCTGAA -3'. With GAPDH as the internal parameter, normalization processing.

2.6. Apoptosis assay

The cells were spread in 6-well plates for 24 h, pretreated with 10 μM JAC4 for 24 h, then treated with 4 Gy X-ray irradiation. After 24 h, the culture medium was abandoned and cells were washed twice with PBS, fixed with cell fixative for 10 min, removed cell

Preprints (www.preprints.org) | NOT PEER-REVIEWED | Posted: 5 June 2023 doi:10.20944/preprints202306.0356.v1

fixative, cleaned twice with PBS, 3 min each time. 1 mL Hoechst 33342 cell staining solution (Beyotime, Shanghai, China) was added to each well and placed in a shaker for staining for 5 min. Discard the dyeing solution and washed with PBS twice, 3 min each time; a drop of anti-fluorescence quencher was then placed in the center of the petri dish and photographed under an inverted fluorescence microscope; and the proportion of apoptotic cells was analyzed. Apoptotic cells were defined as those whose nuclei were fragmented or densely stained. The intact nucleus is a healthy, normal cell. The experiment was carried out at least three times.

2.7. MDA, SOD and CAT assays

The cells were planted on the 6-well plate, treated accordingly, and tested according to the operating instructions of the kits (Beyotime, Shanghai, China).

2.8. Immunofluorescence assay

For immunofluorescence detection, the tissue sections and cells were incubated with primary anti body and then labeled with an anti-rabbit (or mouse) secondary antibody conjugated with Cy3 or FITC (1:1000) in the dark room for 1 h at room temperature. Cell nuclei were counterstained with 40, 60-diamidino-2-phenylindole (DAPI). Images were acquired under a laser scanning confocal microscope (Carl Zeiss Jena) or fluorescence inverted microscope (Nikon). The following antibodies were used: anti-γ-H2AX (1:200, Servicebio, Wuhan, China), anti-P65 (1:200, Santa Cruz, CA, USA), anti-JWA (1:50, AbMax, Beijing, China), anti-TNF-α (1:25, Cell Signaling Technology, USA), anti-TGF-β1 (1:200, Affinity), anti-DNA-PKcs (1:200, Abcam), anti-Ku70 (1:200, Affinity).

2.9. JC-1 staining and reactive oxygen species assay

Mitochondrial membrane potential decline is a landmark event in the early stage of apoptosis. According to the fluorescence probe DCFH-DA entered the cell, the hydrolyzed DCFH was oxidized to produce fluorescent DCF to detect the intracellular ROS level. The cells were planted on six-well plates, treated accordingly, and tested according to the operating instructions of the mitochondrial membrane potential kit (Beyotime, Shanghai, China) and ROS detection kit (Beyotime, Shanghai, China). The intensity of fluorescent staining was quantified with Image J software.

2.10. Colony formation assay

SPCA-1 and BEAS-2B cells were seeded in six-well plates at a density of 500, 1,000 and 1, 500 cells/per well. The cells were treated with 10 μM JAC4 for 24 h and divided into different groups and treated with different doses of radiation (0, 2, 4 or 6 Gy). Fresh medium containing 10 μM JAC4 was replaced every 72 h and incubated in a cell incubator for 8-12 days until colony formation. The plates were then stained with crystal violet (Beyotime, Shanghai, China) and the number of colonies (≥ 50 cells) was counted. Cell colony formation rate, survival fraction and radiosensitization rate were calculated with reference to [28].

2.11. SPCA-1 cell xenograft tumor and radiotherapy mice model

Male nude mice, aged 4-5 weeks, weighing 18-22 g, were purchased from the Model Animal Research Center of Nanjing University (Nanjing, China) and housed in the Laboratory Animal Center of Nanjing Medical University. The mice were fed with food and water AD libitum for 12 h:12 h of night and day, in a SPF clean environment of 25 ± 2 °C and 50 % ± 10 % humidity. The animal study protocol was approved by the Animal Care Committee of Nanjing Medical University (Nanjing, China). After 7 days of acclimatization, SPCA-1 cells (5×10^6) were subcutaneously injected into the right armpit of the mice, level with the upper lung. When the tumor mass reached 60-100 mm^3 (tumor volume = length×width^2/2), the mice were randomly divided into control group, 100 mg/kg JAC4 group (daily administration), 3 Gy×5 fractions X-ray irradiation group (continuous 5 days

Preprints (www.preprints.org) | NOT PEER-REVIEWED | Posted: 5 June 2023 doi:10.20944/preprints202306.0356.v1

of X-ray irradiation), and 100 mg/kg JAC4 + 3 Gy×5 fractions X-ray irradiation group; six mice in each group. RADSOURCE (USA) provided focused beams for localized irradiation of the tumor while ensuring that the whole lung of the mice could be irradiated. Body weight and tumor volume were measured daily. Each tumor tissue was divided into two parts, one half of which was fixed in 4 % paraformaldehyde, and the other half was frozen in a refrigerator at -80 °C for further use. The right lower lobe of each mouse was fixed with 4 % paraformaldehyde, and the remaining lung tissues were frozen in the refrigerator at -80 °C for later use. Routine H&E staining was used for pathological examination of major organs.

2.12. Statistical analysis

GraphPad Prism 8.0 software was used to analyze the experimental data and draw statistical maps. All data are presented as mean ± S.D. One-way-ANOVA and Student's t-test was separately used for comparison between multiple groups and two groups. $p< 0.05$ was considered statistically significant.

3. Results

3.1. JAC4 plays a bidirectional role on the vitality of radiation-treated SPCA-1 and BEAS-2B cells

To determine the effect of X-ray irradiation on the vitality of non-small cell lung cancer cells and normal lung epithelial cells, both SPCA-1 and BEAS-2B cells were exposed to different doses of X-ray. CCK-8 assay showed that 4 Gy and above doses of X-ray irradiation significantly inhibited the vitalities of SPCA-1 and BEAS-2B cells (up to 19.16 % and 25.95 % respectively). With the increase of irradiation dose, the vitalities were dose-dependently reduced in both cells (Figure 1A, B). To determine the optimal dose of JAC4 on SPCA-1 and BEAS-2B cells, we tested the inhibitory effect of JAC4 on cell proliferation. We found that JAC4 suppressed cell proliferation in dose-dependent manner in SPCA1 cells (Figure 1C); however, it did not show similar effect on BEAS-2B cells (Figure 1D). Our previous studies have shown that 10 μM JAC4 is able to prevent the radiation enteritis [26]. Herein, we observed that 10 μM JAC4 treatment slightly increased vitality in BESA-2B cells (Figure 1D). Therefore, we used 10 μM JAC4 and 4 Gy X-ray irradiation for the following experiments.

To further elucidate the effects of JAC4 in combination with RT on SPCA-1 and BEAS-2B cell viabilities, the cells were pretreated with JAC4 for 24 h, and then received X-ray treatment. After 24 h of irradiation, CCK-8 assay showed that the combined treatment (JAC4 plus X-ray) increased suppression of cell viability in SPCA-1 cells. However, the combined treatment alleviated the inhibitory effect on cell viability in BEAS-2B cells (Figure 1E, F). Colony formation data indicated that the combined treatment decreased the clone numbers of SPCA-1 cells (Figure 1G), but partly rescued the clone numbers of BEAS-2B cells from X-ray damages (Figure 1I). The radiotherapy sensitization ratios (SER) were 1.28 and 0.88 in SPCA-1 and BEAS-2B cells, respectively (Figure 1H and J). The results suggested that JAC4 in combination with irradiation increased the toxicity on SPCA-1 cells while reduced the toxicity on BEAS-2B cells.

Preprints (www.preprints.org) | NOT PEER-REVIEWED | Posted: 5 June 2023 doi:10.20944/preprints202306.0356.v1

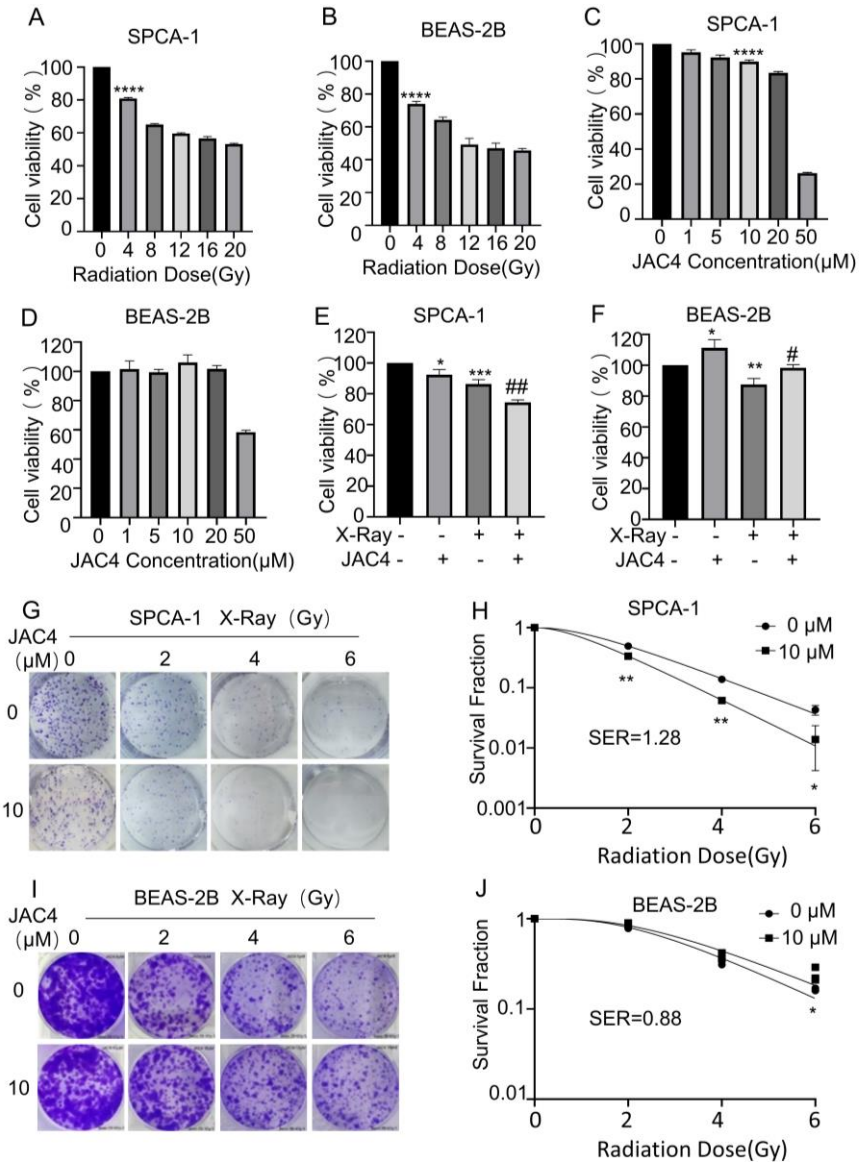

Figure 1. JAC4 plays a bidirectional role in radiation-treated SPCA-1 and BEAS-2B cells. The viabilities of SPCA-1 (A) and BEAS-2B (B) cells exposed to different doses of X-ray irradiation (0, 4, 8, 12, 16, 20 Gy) after 24 h were measured by CCK-8 assay. The viabilities of SPCA-1 (C) and BEAS-2B (D) cells exposed to different doses of JAC4 (1, 5, 10, 20, 50 μM) or DMSO after 24 h were measured by CCK-8 assay. SPCA-1 (E) and BEAS-2B (F) cells were pretreated with JAC4 (10 μM) or DMSO for 24 h and then exposed to X-ray irradiation (4 Gy). After 24 h, the viabilities of cells were measured by CCK-8 assay. The radiosensitivities of JAC4 (10 μM) on SPCA-1(G) and BEAS-2B (I) cells treated with the indicated X-ray irradiation doses (0, 2, 4, 6 Gy) were evaluated by colony formation assay. The surviving fractions of SPCA-1 (H) and BEAS-2B (J) cells were calculated as described. Data are presented as the mean ± SD (n=3); (* $p< 0.05$, ** $p< 0.01$, *** $p< 0.001$, **** $p< 0.0001$, vs. control group and # $p< 0.05$, ## $p< 0.01$, vs. the X-ray irradiation group).

3.2. JAC4 increases DSBs and apoptosis after RT in SPCA-1 cells, while reduces the effects in normal cells

To determine if JAC4 differentially regulates X-ray triggered DNA damage in both SPCA-1 and BEAS-2B cells, the expression of γ-H2AX was detected in both cells. The Western blotting results showed that γ-H2AX expression in SPCA-1 cells was increased dose-dependently after X-ray (0, 2, 4, 8 Gy) exposure; and it was time-dependently reduced at 0.5, 6 and 24 h after irradiation (Figure S1A). Further data showed a significant accumulation of γ-H2AX was observed at 4 Gy in both cells; and the protein level of γ-H2AX at 0.5 h was 4.3-fold higher than that at 6 h after irradiation in SPCA-1 cells (Figure

 doi:10.20944/preprints202306.0356.v1

S1B). Interestingly, the cumulative peak of γ-H2AX was observed at 2 h in SPCA-1 cells but at 0.5 h to 2 h continuously in BEAS-2B cells after irradiation (Figure S1C). Based on above data, the γ-H2AX foci and protein expression were examined at 2 h after irradiation in later models. The immunofluorescence and Western blotting assays showed that compared to control group, X-ray treatment increased γ-H2AX foci intensity and the expression of γ-H2AX; JAC4 in combination with X-ray treatment enhanced γ-H2AX foci intensity and protein expression in SPCA-1 cells but reduced the both levels in BEAS-2 cells (Figure 2A-D).

We also completed Hoechst 33342 apoptosis assay. Compared with irradiation treatment alone, JAC4 in combination with X-ray treatment enhanced the pro-apoptotic toxicity in SPCA-1 cells (Figure 2E, F). In contrast, JAC4 reduced the pro-apoptotic toxicity of irradiation in BEAS-2 cells (Figure 2E, G). The decline of mitochondrial membrane potential is known a hallmark event in the early stage of apoptosis. Mitochondrial membrane potential was measured by fluorescent probe JC-1. Red fluorescence indicates the formation of JC-1 aggregates due to high mitochondrial membrane potential, while green fluorescence indicates the depolarized mitochondrial membrane potential. The ratio of red to green fluorescence represents the number of early apoptotic cells. Data showed that JAC4 in combination with X-ray treatment reduced mitochondrial membrane potential in SPCA-1 cells (Figure 2H, I). In contrast, JAC4 reversed the reduction of mitochondrial membrane potential in BEAS-2B cells by irradiation (Figure 2H, J). Therefore, JAC4 increased radiation-induced DNA damage and apoptosis in SPCA-1 cells while partly protected BEAS-2B cells from X-ray triggered DNA damage and apoptosis.

Preprints (www.preprints.org) | NOT PEER-REVIEWED | Posted: 5 June 2023 doi:10.20944/preprints202306.0356.v1

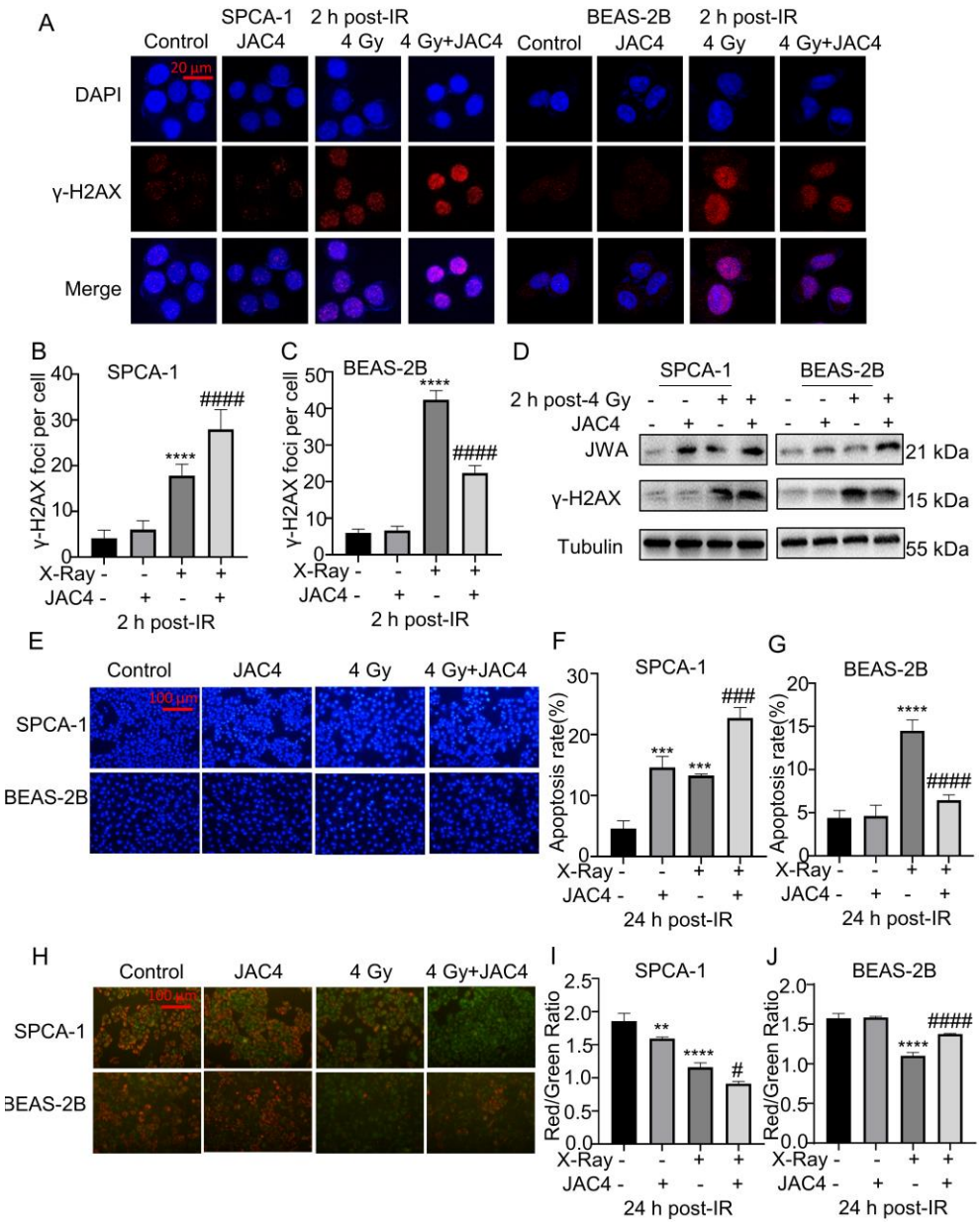

Figure 2. JAC4 enhances radiation toxicity to SPCA-1 but reduces radiation toxicity to BEAS-2B cells. (A) The formation of γ-H2AX foci was determined by immunofluorescence assay at 2 h after 4 Gy of X-ray irradiation. The images of SPCA-1 cells are on the left panel, and the BEAS-2B cells are on the right panel. γH2AX (red) and DAPI (blue). The number of γ-H2AX foci of SPCA-1 (B) and BEAS-2B (C) cells were counted as described. (Scale bar, 20 μm) (D) The Western blotting images of γ-H2AX and JWA in SPCA-1 and BEAS-2B cells at 2 h after 4 Gy of X-ray irradiation. (E) SPCA-1 and BEAS-2B cells were pretreated with JAC4 (10 μM) or DMSO for 24 h and then exposed to X-ray irradiation (4 Gy). the Hoechst staining images in SPCA-1 and BEAS-2B cells. (Scale bars, 100 μm). (F-G) The quantitative data of apoptosis ratios. (H) JC-1 staining in SPCA-1 and BEAS-2B cells (Scale bars, 100 μm). (I-J) The ratio of red to green fluorescence intensity. Data are presented as the mean ± SD (n=3); (** $p< 0.01$, *** $p< 0.001$, **** $p< 0.0001$, vs. control group and # $p< 0.05$, ### $p< 0.001$, #### $p< 0.0001$, vs. the X-ray irradiation group).

3.3. JAC4 differentially regulates HR and NHEJ signal pathways in SPCA-1 and BEAS-2 cells

To elucidate if JAC4 via both HR and NHEJ signal pathways to differentially regulate DNA repair in SPCA-1 and BEAS-2B cells after X-ray exposure, we further detected the NHEJ biomarkers DNA-PKcs and Ku70, and HR biomarkers p-ATR and p-CHK1, respectively. JAC4 treatment alone slightly reduced the expressions of DNA repair proteins in SPCA-1. Accordingly, compared to the X-ray treatment alone, JAC4 in combination with

Preprints (www.preprints.org) | NOT PEER-REVIEWED | Posted: 5 June 2023 doi:10.20944/preprints202306.0356.v1

X-ray exposure increased the levels of γ-H2AX but reduced DNA-PKcs, Ku70, p-ATR, p-CHK1 in SPCA-1 cells (Figure 3A). However, the level of γ-H2AX was reduced and the DNA repair proteins were barely changed in BEAS-2B cells (Figure 3B). The RNA-seq datasets (GSE18842) from GEO database confirmed that in NSCLC patients (n=46), the expression of JWA gene was negatively correlated with DNA-PKcs and CHK1 genes (Figure 3C, D). These data suggested that JAC4 differentially regulated NHEJ and HR signaling pathways in SPCA-1 and BEAS-2B cells.

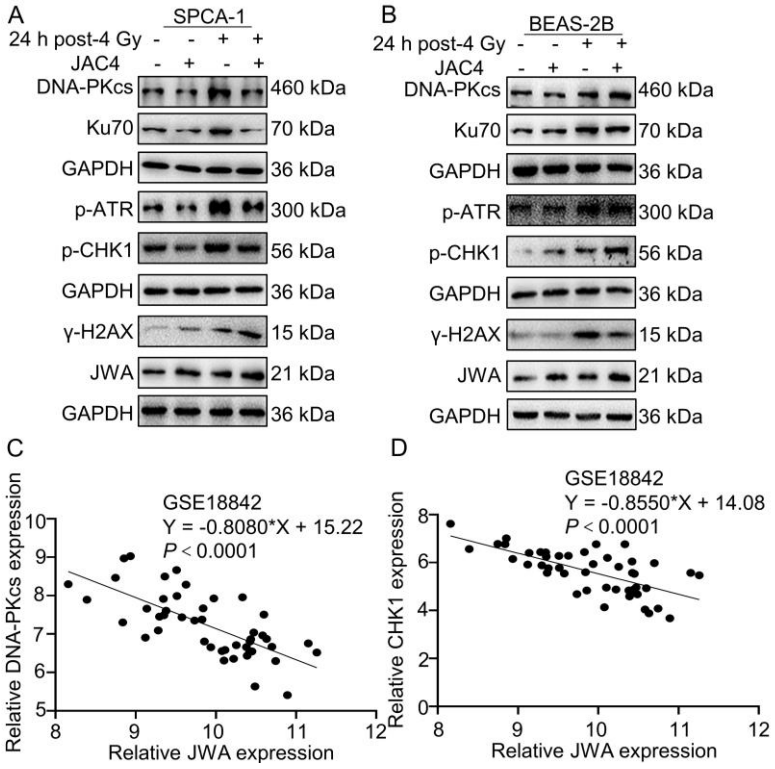

Figure 3. JAC4 differentially regulates NHEJ and HR pathways in SPCA-1 and BEAS-2B cells. (A-B) The Western blotting images of DNA-PKcs, Ku70, p-ATR, p-CHK1, γ-H2AX, JWA and GAPDH in SPCA-1 and BEAS-2B cells at 24 h after 4 Gy of X-ray irradiation. (C-D) GSE18842 (Number of patients with NSCLC=46) database was analyzed for the correlation between JWA and DNA-PKcs and CHK1 mRNA expression.

3.4. JAC4 alleviates the oxidative stress and prevents NF-κB nuclear translocation in BEAS-2B cells

Irradiation induces a large number of ROS and oxidative stress reaction and results in DNA damage [29]. ROS content was detected by fluorescent probe DCFH-DA. The results showed that irradiation induced ROS intensity in SPCA-1 cells was obviously increased but it was reduced in BEAS-2B cells after in combination with JAC4 treatment (Figure 4A, B). Correspondingly, the combined treatment also partly reversed the levels of SOD, CAT and MDA in BEAS-2B cells compared to X-ray treatment alone (Figure 4 C-E).

The production of ROS activates NF-κB and promotes its translocation to the nucleus. The immunofluorescence assay demonstrated that irradiation triggered the nuclear translocation of NF-κB in BEAS-2B cells were obviously prevented in the combined treatment of RT and JAC4 (Figure 4F). The Western blotting data further confirmed that JAC4 prevented irradiation increased nuclear NF-κB in BEAS-2B cells (Figure 4G). These data were consistent with our previous results [30]. Suggest that JAC4 alleviated irradiation-induced oxidative stress and prevented NF-κB nuclear translocation.

Preprints (www.preprints.org) | NOT PEER-REVIEWED | Posted: 5 June 2023 doi:10.20944/preprints202306.0356.v1

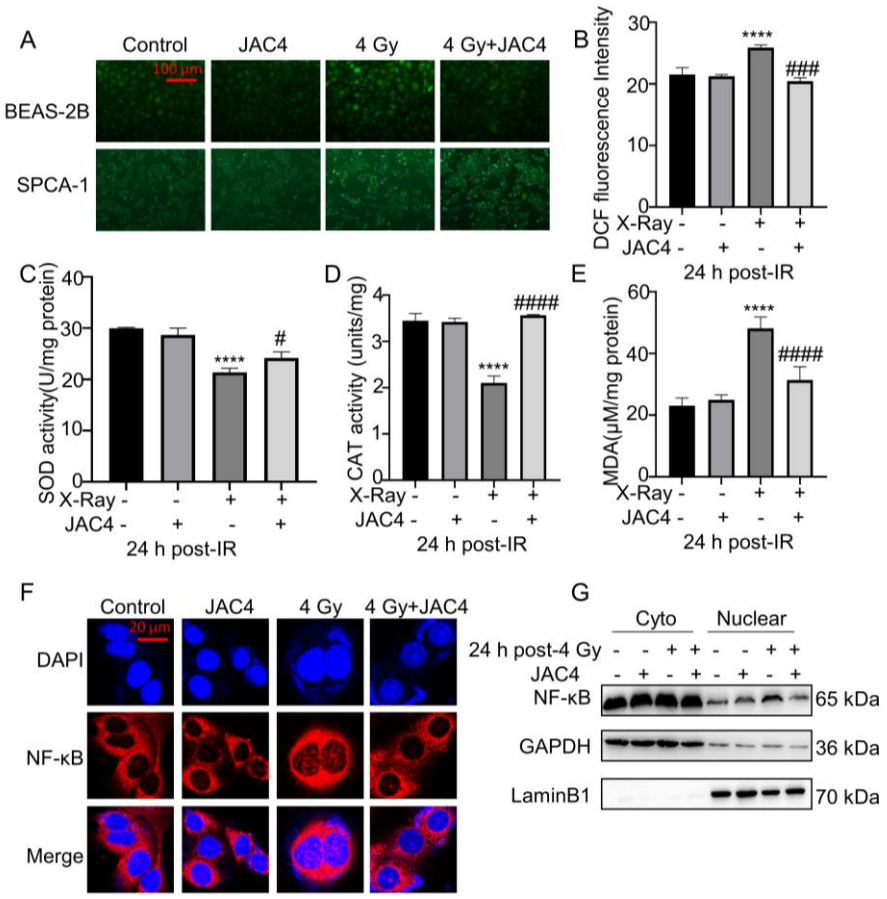

Figure 4. JAC4 enhances the antioxidant capacity of BEAS-2B cells induced by irradiation. BEAS-2B and SPCA-1 cells were pretreated with JAC4 (10 μM) or DMSO for 24 h and then exposed to X-ray irradiation (4 Gy). (A) The intracellular ROS test images of SPCA-1 and BEAS-2B cells (Scale bars, 100 μm). (B) The ROS fluorescence intensity analysis in BEAS-2B cells. (C-E) The activity of SOD, CAT and the level of MDA in BEAS-2B cell lysates. (F)The immunofluorescence staining of P65 in BEAS-2B cells (Scale bars, 20 μm). (G) Nuclear-cytoplasmic separation Western blotting assay was carried out to confirm the position change of P65 protein in BEAS-2B cells. Data are presented as the mean ± SD (n=3); (**** $p< 0.0001$, vs. control group and # $p< 0.05$, ### $p< 0.001$, #### $p< 0.0001$, vs. the X-ray irradiation group).

3.5. Knockdown of JWA attenuates the effect-enhancing and toxicity-reducing effects of JAC4 plus X-ray in SPCA-1 and BEAS-2B cells

To clarify if the bidirectional roles of JAC4 were mediated by targeted activation of JWA gene, both SPCA-1 and BEAS-2B cells were transfected with siJWA, respectively. Compared with sicontrol plus JAC4 group, the immunofluorescence assay showed that the γ-H2AX foci was decreased in siJWA plus JAC4 group in SPCA-1 cells but increased in BEAS-2B cells at 24 h post-irradiation (Figure 5A-C). Western blotting assay showed that the expression levels of JWA were lower, and the expressions of p-p65, γ-H2AX were higher in siJWA plus JAC4 group compared with sicontrol alone and sicontrol plus JAC4 group in BEAS-2B cells (Figure 5D); however, the expression levels of both JWA and γ-H2AX were lower, and the expressions of DNA-PKcs, Ku70, p-ATR and p-CHK1 were higher in siJWA plus JAC4 group in SPCA-1 cells compared to the sicontrol plus JAC4 treated group (Figure 5E). Colony formation assay showed that compared with the sicontrol plus JAC4 group, the clone numbers in the siJWA plus JAC4 group was increased in SPCA-1 cells, but decreased in BEAS-2B cells (Figure 5F-I). All these results suggested that the bidirectional roles of JAC4 on RT were mediated by activation of JWA in both SPCA-1 and BEAS-2B cells.

Preprints (www.preprints.org) | NOT PEER-REVIEWED | Posted: 5 June 2023 doi:10.20944/preprints202306.0356.v1

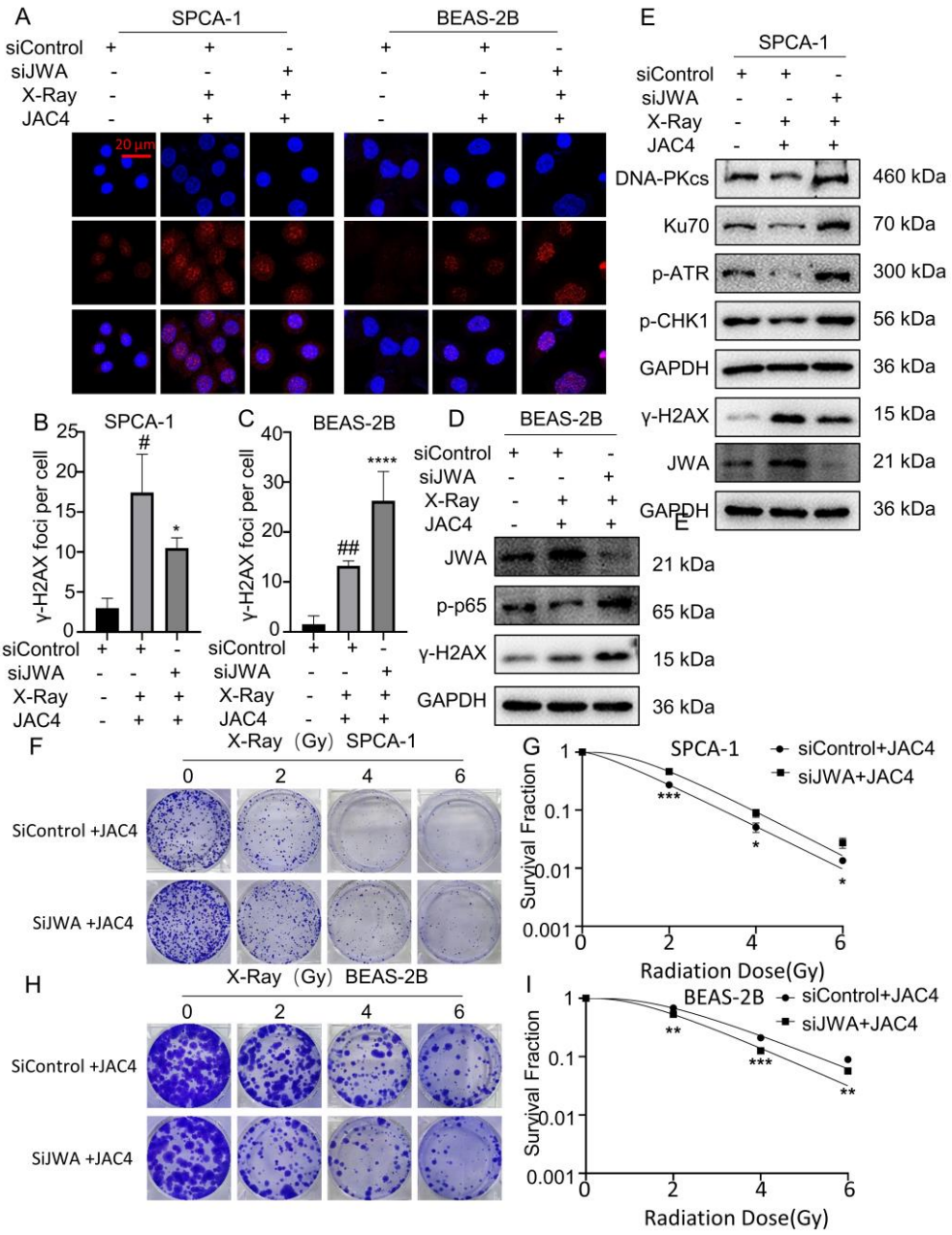

Figure 5. Knockdown of JWA mitigates damages of X-ray on SPCA-1 but enhances the inju ries on BEAS-2B cells. (A) γ-H2AX foci were tested by immunofluorescence assay in SPCA-1 and BEAS-2B cells transfected with sicontrol, sicontrol plus JAC4 and siJWA plus JAC4 groups 24 h after irradiation. The number of γ-H2AX foci of SPCA-1 (B) and BEAS-2B (C) cells were counted as described (Scale bar, 20 μm). (D) Protein levels of JWA, γ-H2AX and p-p65 in BEAS-2B cells of each group 24 h post-X-ray. (E) Protein levels of JWA, γ-H2AX, DNA-PKcs etc. in SPCA-1 cells of each group 24 h post-X-ray. (F-I) The radiosensitivity of JWA knockdown in SPCA-1 and BEAS-2B cells was verified by colony formation assay after the cells were irradiated with different doses (0, 2, 4 or 6 Gy). (n=3); (* $p< 0.05$, ** $p< 0.01$, *** $p< 0.001$, **** $p< 0.0001$ vs. sicontrol group and # $p< 0.05$, ## $p< 0.01$ vs. the siJWA plus JAC4 group).

3.6. JAC4 exerts effect-enhancing and toxicity-reducing of RT on lung cancer in vivo

To confirm the effect-enhancing and toxicity-reducing role of JAC4 in combination with X-ray *in vivo*, a xenograft mouse model was constructed with SPCA-1 cells (Figure 6A). To mimic the real environment of *in vivo* X-ray therapy, the entire lung was irradiated at the same time as the tumor site (Figure 6B). Tumor volumes in JAC4 or irradiation alone treatment group were smaller than that in the control group, while the combined treatment showed a synergistic effect on tumor suppression (Figure 6C, D). The ratio of tumor

Preprints (www.preprints.org) | NOT PEER-REVIEWED | Posted: 5 June 2023 doi:10.20944/preprints202306.0356.v1

to body weight of mice was significantly lower in combined treatment group than that in irradiation alone group (Figure 6E). Compared with the control group, tumor inhibition rates in JAC4 alone, irradiation alone and the combined treatment were 25.45%, 49.95% and 78.05%, respectively (Figure 6F). In the present study, there was no significant changes in body weight of model mice among various treatment groups and no death of mice was observed during the experiment. The body weight curve of mice in JAC4 group was completely overlapped with that of control mice (Figure S2A). In addition, H&E staining showed that JAC4 in combination with irradiation caused more necrotic area of tumor tissue than the other groups (Figure S2B). Western blotting showed that compared to irradiation group, the combined treatment induced higher γ-H2AX protein level and lower DNA-PKcs, Ku70 and p-ATR (Figure 6G-L). The immunofluorescence assay displayed the similar data with Western blotting assay (Figure S2D).

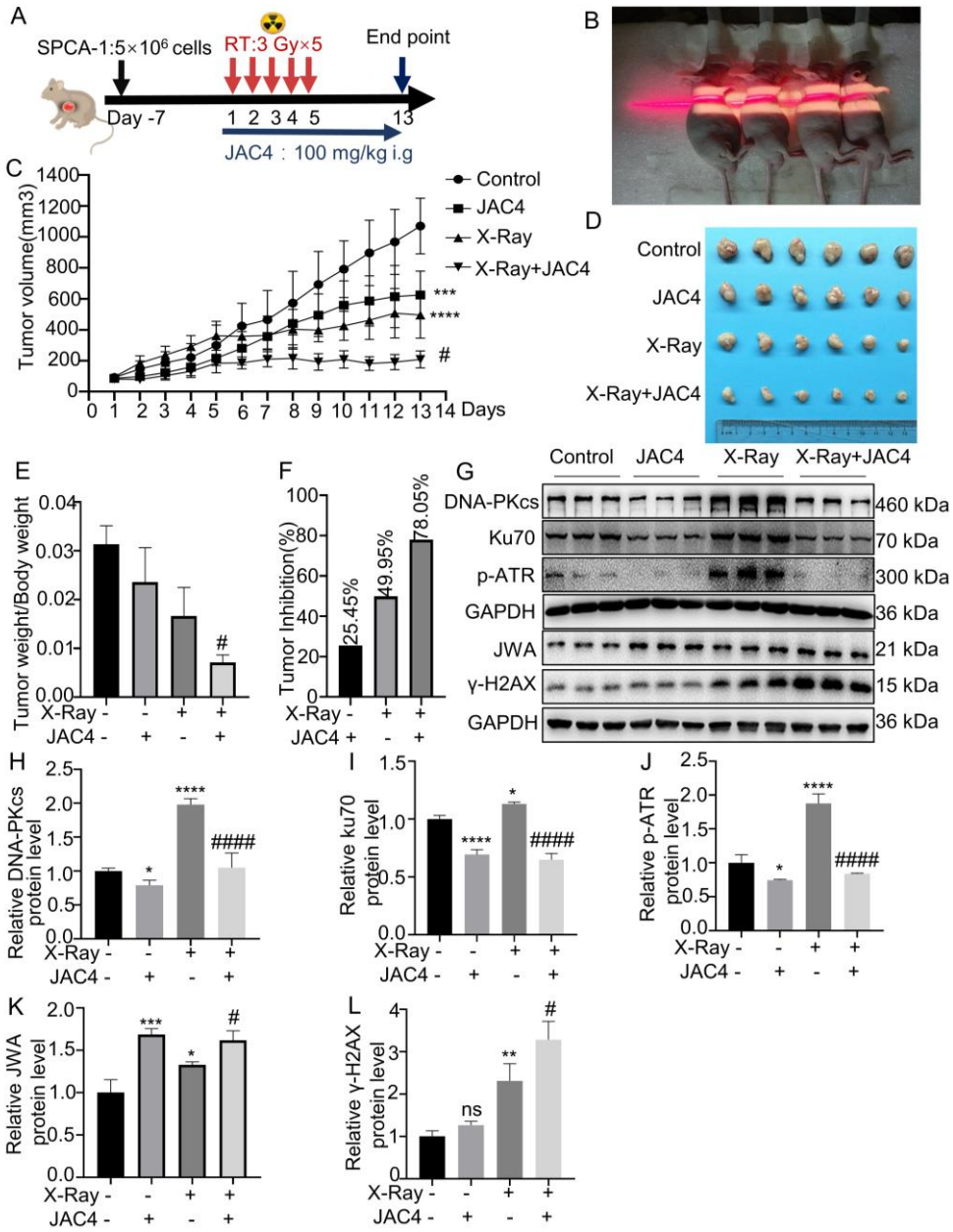

Figure 6. JAC4 has a synergistic effect on X-ray-treated tumors *in vivo*. (A) Once the xenograft tumors reached specific volume, the mice were given oral JAC4 (100 mg/kg, once a day until the model end), and irradiated (3 Gy×5 fractions). (B) Irradiation therapy image (the irradiated areas included mice with subcutaneous tumors and the whole chest). (C) The tumor growth curves of xenograft model in control, JAC4, X-Ray and the combined groups (n=6). (D) Image of tumors in each group

Preprints (www.preprints.org) | NOT PEER-REVIEWED | Posted: 5 June 2023 doi:10.20944/preprints202306.0356.v1

of mice. (E) The ratio of tumor weight to body weight on day 13. (F) The tumor inhibition rate in each group. (G) The Western blotting images of DNA-PKcs, Ku70, p-ATR, JWA and γ-H2AX in tumor tissues. (H-L) Quantification of DNA-PKcs, Ku70, p-ATR, JWA and γ-H2AX protein levels in tumor tissues. Data are presented as the mean ± SD (n=3); (* $p< 0.05$, ** $p< 0.01$, *** $p< 0.001$, **** $p< 0.0001$ vs. control group and # $p< 0.05$, ## $p< 0.01$, ### $p < 0.001$ vs. the X-ray irradiation group).

The lung is known radiosensitive organ. NSCLC RT usually causes inflammatory response in the lung [31]. H&E staining showed that irradiation treatment resulted in obvious inflammatory cell infiltrations in lung tissues, whereas the combined treatment reduced the lung inflammation (Figure 7A). In addition, qRT-PCR results showed that JAC4 reversed IL-10, TNF-α, TGF-β1 and IL-1β mRNA levels of lung tissues induced by irradiation (Figure 7B-E). Western blotting assay showed that compared to irradiation treatment alone, the combined treatment increased JWA protein level but reduced γ-H2AX and p-p65 protein levels (Figure 7F-I). Moreover, immunofluorescence assay showed that the combined treatment decreased the fluorescence intensity of TNF-α and TGF-β1 (Figure S2C). All these data confirmed the bidirectional effects of JAC4 in synergistically increasing toxicity on cancer and reducing radiotoxicity on normal lung tissue during NSCLC RT.

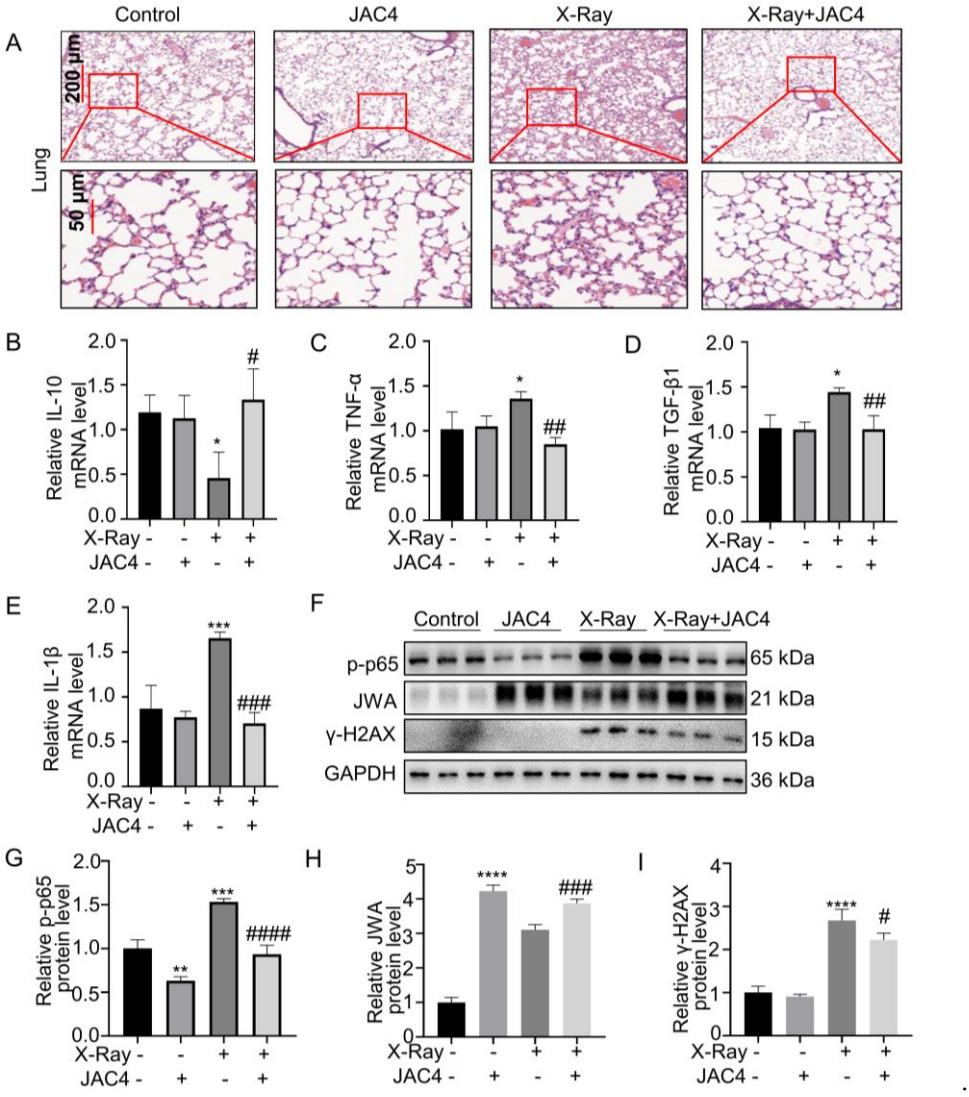

Figure 7. JAC4 inhibits X-ray-induced inflammatory and injury of lung tissues *in vivo*. (A) H&E staining of lung tissues in each group. (B-E) The mRNA levels of IL-10, TNF-α, TGF-β1 and IL-1β in lung tissues were determined by qRT-PCR assay. (F) The Western blotting images of JWA, γ-H2AX and p-p65 protein in lung tissues. (G-I) Quantification of p-p65, JWA and γ-H2AX protein levels in

Preprints (www.preprints.org) | NOT PEER-REVIEWED | Posted: 5 June 2023 doi:10.20944/preprints202306.0356.v1

lung tissue. Data are presented as the mean ± SD (n=3); (ns: $p > 0.05$; * $p < 0.05$, ** $p < 0.01$, *** $p < 0.001$, **** $p < 0.0001$ vs. control group; # $p < 0.05$, ### $p < 0.001$, #### $p < 0.0001$ vs. the X-ray irradiation group).

4. Discussion

RT is one of the main treatments for most cancers including NSCLC. Due to the rapid repair of DSBs in tumor tissue, cancer tissue can survive for a long time. There are few radiosensitizers that can simultaneously enhance efficacy and attenuate toxicity in RT. In this study, we reported for the first time that JAC4 has a synergistic and attenuate effect in RT for NSCLC. On the one hand, JAC4 enhanced the killing effect of RT on NSCLC both *in vitro* and *in vivo*. On the other hand, JAC4 reduced the toxic effect of RT on normal lung tissue. The mechanistic evidence showed that JAC4 promoted apoptosis in NSCLC by blocking ATR-CHK1 and DNA-PKcs and further inhibited DNA repair therefore increased DNA double-strand damage (Figure 8A). In addition, JAC4 enhanced antioxidant, anti-inflammatory abilities and prevented NF-κB nuclear translocation therefore attenuated radiation induced oxidative stress and inflammation in normal lung tissue (Figure 8B). Our study may provide a new valuable target and strategy for lung cancer RT.

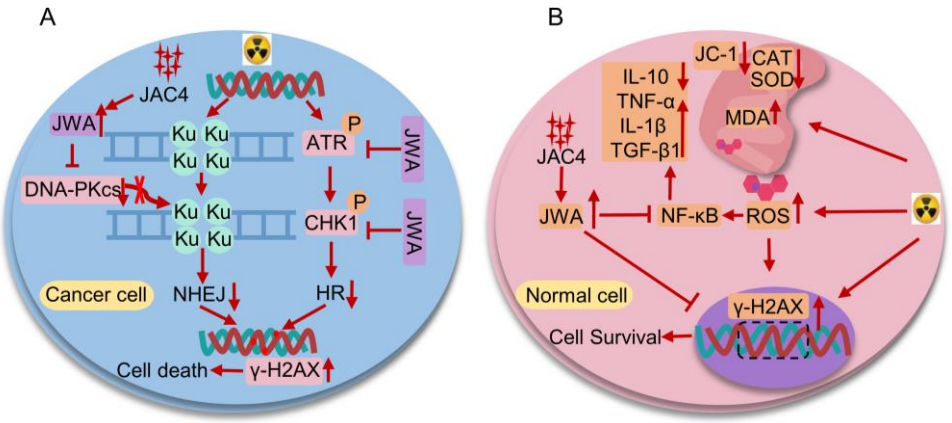

Figure 8. The bidirectional mechanisms diagram of JAC4 in combination with radiotherapy for lung cancer. (A) Mechanism of action how JAC4 increases damages of X-ray on lung cancer cells. (B) Mechanism of action how JAC4 reduces damages of X-ray on normal lung epithelial cells.

RT resistance of NSCLC is closely related to PI3K-AKT, HGF-cMet, cGAS-STING, HR and NHEJ signaling pathways [32-35]. A number of studies have shown that radiosensitizers that inhibit DNA double-strand break repair molecules can increase efficacy of RT on lung cancer [36-38]. ATR is activated by TopBP1 or ETAA1 is recruited to RPA-ssDNA, phosphorylates and activates CHK1 to cause cell cycle arrest, leaving sufficient time for DNA damage to be checked and repaired [39]. Ku binds to DNA-PKcs and triggered by DNA double-strand damage caused by radiation. Self-phosphorylation of DNA-PKcs changes its conformation and releases it from the DNA double-strand, resulting in NEHJ [40]. In this study, JAC4 inhibited the expression of ATR/CHK1 and DNA-PKcs/Ku70 proteins by activating JWA gene expression, which increased DSBs and promoted apoptosis in lung cancer cells. In NSCLC, JWA and topoisomerase IIα have a negative feedback regulation on each other, and inhibition of topoisomerase IIα will lead to increase DNA damage [20, 41]. In this study, JAC4 in combination with RT increased expression of JWA gene and inhibited the expression of ATR/CHK1 in NSCLC, which may be related to topoisomerase IIα. How JWA inhibits the expression of DNA-PKcs in NSCLC needs to be further elucidation.

JWA maintains redox homeostasis and suppresses inflammation process by inhibition of NF-κB to reduce ROS production [30]. SOD is known enzyme that directly remove free radicals [42]. SOD converts oxygen radicals into hydrogen peroxide. Catalase (CAT) decomposes hydrogen peroxide into water and oxygen molecules and is an important antioxidant [43]. MDA is the product of peroxidation of polyunsaturated fatty acids, and

 doi:10.20944/preprints202306.0356.v1

the production of ROS can cause the production of MDA [44]. Ionizing radiation produces a large number of various ROS in the body, resulting in oxidative stress and inflammatory reactions [45]. Continuous ROS and oxidative stress cause DNA double-strand damage. Therefore, antioxidant system plays important role in the prevention and treatment of RP. In this study, after JAC4 treatment, JWA was activated to prevent the translocation of NF-κB into nucleus in normal cells, and the levels of ROS, MDA, pro-inflammatory factor TGF-β1, TNF-α and IL-1β were significantly decreased and the levels of SOD, CAT and anti-inflammatory factor IL-10 were increased in normal BEAS-2B cells, therefore obviously reduced irradiation induced DNA damages in normal cells. Studies have shown that inhibiting the activation of NF-κB can also enhance the sensitivity of RT to cancer cells [46]. NF-κB may be the key point of bidirectional effect of JAC4 in protection of normal lung tissue from RT induced damage.

In lung tissue, ROS production is derived from multiple cells including endothelial cells, neutrophils, eosinophils, alveolar macrophages, and alveolar epithelial cells. The results of this study indicated that JAC4 inhibited ROS production in lung tissue, but the specific cell type targeted by JAC4 need to further identified. At present, the diagnosis of radiation-induced lung injury is still limited to early treatment and typical clinical manifestations [47, 48], and lacks early predictive biomarkers. Our results showed that JAC4 through activation of JWA to alleviate radiation-induced oxidative stress, inflammation and DNA damages in lung tissues; at the same time, JAC4 enhances RT induced DNA damage and apoptosis in lung cancer cells. Therefore, whether JAC4 can be used as a protective agent for early intervention of radioactive lung injury; more importantly, further studies are needed to confirm whether the combination of JAC4 and radiotherapy can properly increase the radiation dose to further improve the therapeutic effect on lung cancer.

Single cell transcriptomics analysis indicate that many genes involved in mitochondrial depolarization are upregulated by RT, which may activate the cGAS-STING signaling pathway [49]. In our study, JAC4 showed significantly different effects on RT-triggered mitochondrial membrane potential depolarization between SPCA-1 and BEAS-2B cells. This suggests that depolarization of mitochondrial membrane potential may be another key point of JAC4 bidirectional effect. It is well documented that cGAS-STING signaling pathway presents different expression states in cancer cells and normal lung tissues. Activation of cGAS-STING pathway enhances the radiosensitivity of NSCLC cells [34]. Inhibition of cGAS-STING pathway can also be used to reduce radiation-induced lung injury [50]. There is much evidence that some signal regulatory pathways are shared between cancer and normal cells, but the effects on phenotypes may be completely opposite, which is mostly due to the differential microenvironment between cancer and normal tissues. JWA may achieve the biological function of maintaining homeostasis by differentially regulating lung cancer cells and normal lung tissue cells damaged by radiation. Whether the bidirectional effects of JAC4 is related to the cGAS-STING pathway needs to be further clarified.

In conclusion, the synergistic and attenuated effects of JAC4 in NSCLC radiotherapy have been confirmed both *in vitro* and *in vivo* models. JWA differential regulation of oxidative stress and DNA repair in cancer and normal cells induced by radiotherapy is the key event for the bidirectional effect of JAC4 in combination with radiotherapy. The evidence from this study may provide translational new strategies for optimizing radiation therapy for lung cancer.

Preprints (www.preprints.org) | NOT PEER-REVIEWED | Posted: 5 June 2023 doi:10.20944/preprints202306.0356.v1

Supplementary Materials:

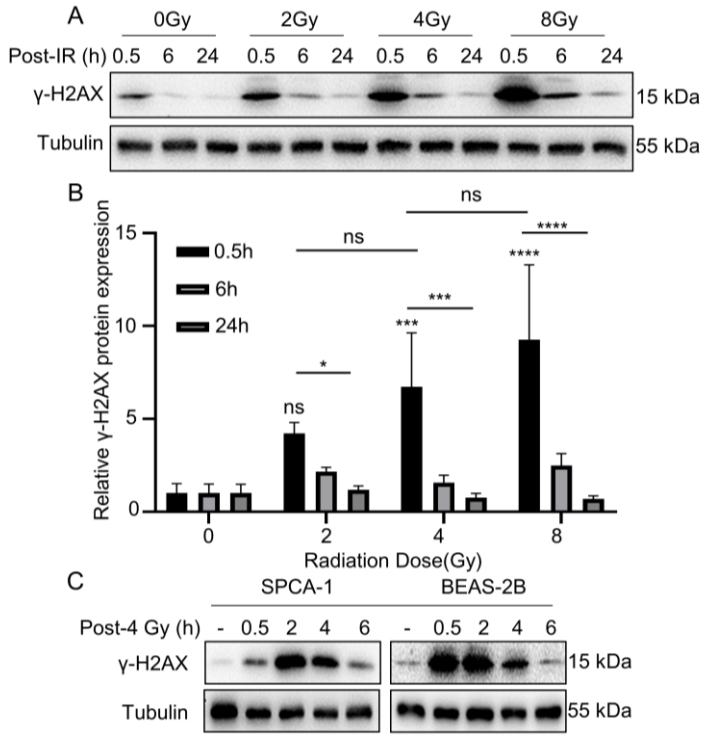

Figure S1. Time- and dose-effect relationship of X-ray irradiation on DSBs in SPCA-1 and BEAS-2B cells. (A) The Western blotting images of γ-H2AX and tubulin in SPCA-1 cells at different time points (0.5, 6, 24 h) after X-Ray irradiation (0, 2, 4, 8 Gy). (B) Quantification of γ-H2AX protein levels in SPCA-1 cells. (C) Western blotting images of γ-H2AX and tubulin in SPCA-1 and BEAS-2B cells at different time points (0.5, 2, 4, 6h) after X-ray irradiation (4 Gy). Data are presented as the mean ± SD (n=3); (ns: $p > 0.05$; * $p < 0.05$, *** $p < 0.001$, **** $p < 0.0001$, vs. control or specific groups).

Preprints (www.preprints.org) | NOT PEER-REVIEWED | Posted: 5 June 2023 doi:10.20944/preprints202306.0356.v1

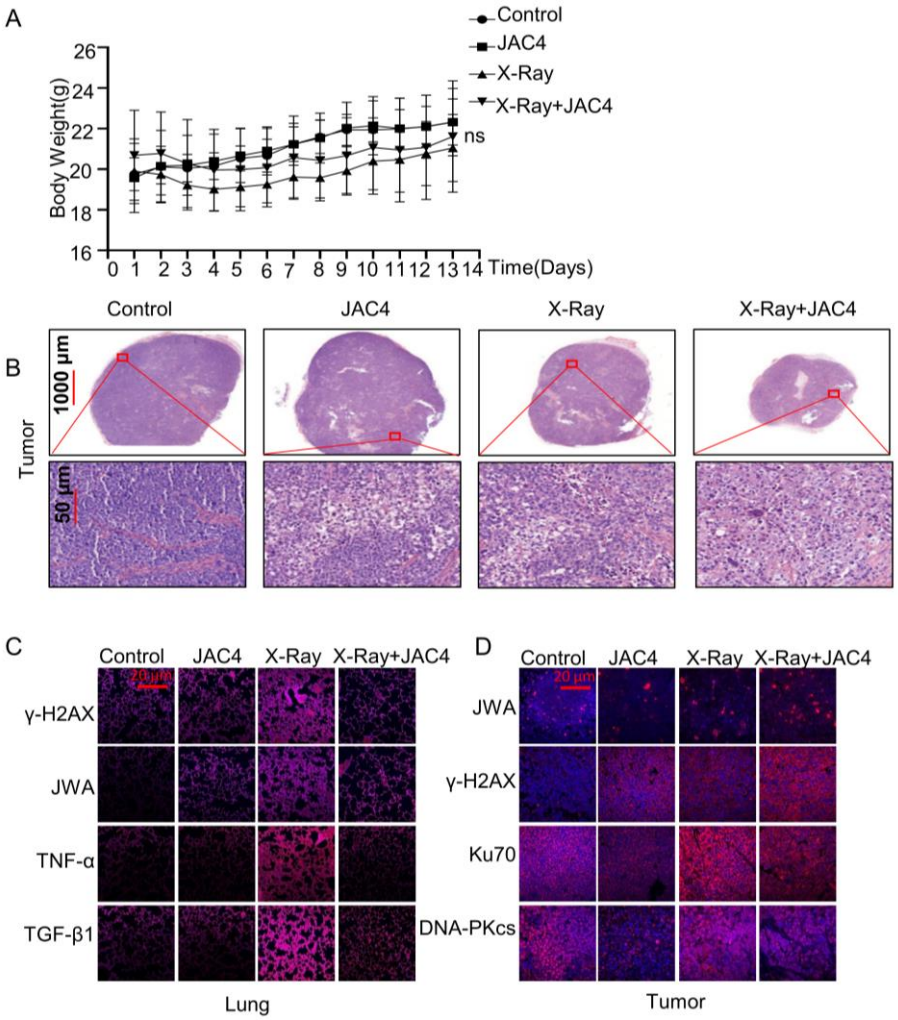

Figure S2. JAC4 exerts synergistic and attenuated effects *in vivo*. (A) The body weight growth curves of xenograft model mice in each group. (B) H&E staining of lung tissues in each group. (C) Immunofluorescence staining of γ-H2AX, JWA, TNF-α and TGF-β1 in lung tissues of each group. (D) Immunofluorescence staining of JWA, γ-H2AX, Ku70, DNA-PKcs, in tumor tissues of each group. (Scale bar, 20 μm). .

Author Contributions: Conceptualization and P.I.; J.Z. Development of methodology: L.W., J.N. and K.D.; acquisition of data. L.W. and J.N.; analysis and interpretation of data: L.W., J.N., K.D., and C.Z.; writing, review, and/or revision of the manuscript: L.W. and J.Z.; administrative, technical, or material support: L.W., J.N., K.D. and A.L. All authors have read and agreed to the published version of the manuscript.

Funding: This study was supported by the National Natural Science Foundation of China (Nos.81973156, 81673219 to J.Z.).

Institutional Review Board Statement: This study followed the guidelines for the care and use of laboratory animals. The Animal Care and Use Institutional Committee of Nanjing Medical University approved all procedures in this study (IACUC-2012059).

Informed Consent Statement: Not applicable.

Data Availability Statement: The data is contained within the article and Supplementary Materials.

Conflicts of Interest: The authors declare no conflict of interest.

 doi:10.20944/preprints202306.0356.v1

References

1. Sung, H.; Ferlay, J.; Siegel, R.L.; Laversanne, M.; Soerjomataram, I.; Jemal, A.; Bray, F. Global cancer statistics 2020: GLOBOCAN estimates of incidence and mortality worldwide for 36 cancers in 185 countries. *CA. Cancer J. Clin.* 2021, 71, 209-249.

2. Shirley, M.; Keam, S.J. Aumolertinib: a review in non-small cell lung cancer. *Drugs.* 2022, 82, 577-584.

3. Kumar, M.; Sarkar, A. Current therapeutic strategies and challenges in NSCLC treatment: a comprehensive review. *Exp. Oncol.* 2022, 44.

4. Miller, M.; Hanna, N. Advances in systemic therapy for non-small cell lung cancer. *BMJ.* 2021, 375, n2363.

5. Rodríguez De Dios, N.; Navarro-Martin, A.; Cigarral, C.; Chicas-Sett, R.; García, R.; Garcia, V.; Gonzalez, J.A.; Gonzalo, S.; Murcia-Mejía, M.; Robaina, R.; et al. GOECP/SEOR radiotheraphy guidelines for non-small cell lung cancer. *World J. Clin. Oncol.* 2022, 13, 237-266.

6. Choi, Y.; Noh, J.M.; Shin, S.H.; Lee, K.; Um, S.W.; Kim, H.; Pyo, H.; Ahn, Y.C.; Jeong, B.H. The incidence and risk factors of chronic pulmonary infection after radiotherapy in patients with lung cancer. *Cancer Res. Treat*. 2023.

7. Césaire, M.; Montanari, J.; Curcio, H.; Lerouge, D.; Gervais, R.; Demontrond, P.; Balosso, J.; Chevalier, F. Radio-resistance of non-small cell lung cancers and therapeutic perspectives. *Cancers.* 2022, 14.

8. Huang, R.X.; Zhou, P.K. DNA damage response signaling pathways and targets for radiotherapy sensitization in cancer. Signal. Transduction. *Targeted Ther.* 2020, 5, 60.

9. Santivasi, W.L.; Xia, F. Ionizing radiation-induced DNA damage, response, and repair. *Antioxid*. *Redox Signal.* 2014, 21, 251-259.

10. Liu, Y.P.; Zheng, C.C.; Huang, Y.N.; He, M.L.; Xu, W.W.; Li, B. Molecular mechanisms of chemo- and radio therapy resistance and the potential implications for cancer treatment. *Med. Comm.* 2021, 2, 315-340.

11. Simone, C.B. Thoracic radiation normal tissue injury. *Semin. Radiat. Oncol.* 2017, 27, 370-377.

12. Liu, T.; Zhang, L.; Joo, D.; Sun, S.-C. NF-κB signaling in inflammation signal transduction. *Targeted. Ther.* 2017, 2, 17023-17023.

13. Verma, S.; Dutta, A.; Dahiya, A.; Kalra, N. Quercetin-3-rutinoside alleviates radiation-induced lung inflammation and fibrosis via regulation of NF-κB/TGF-β1 signaling. *Phytomedicine: Int. J. Phytother. Phytopharm*. 2022, 99, 154004.

14. Wang, S.; Gong, Z.; Chen, R.; Liu, Y.; Li, A.; Li, G.; Zhou, J. JWA regulates XRCC1 and functions as a novel base excision repair protein in oxidative-stress-induced DNA single-strand breaks. *Nucleic Acids Res*. 2009, 37, 1936-1950.

15. Ding, K.; Liu, X.; Wang, L.M.; Zou, L.; Jiang, X.Q.; Li, A.P.; Zhou, J.W. Targeting JWA for cancer therapy: functions, mechanisms and drug discovery. *Cancers.* 2022, 14.

16. Ye, Y.; Li, X.; Yang, J.; Miao, S.; Wang, S.; Chen, Y.; Xia, X.; Wu, X.; Zhang, J.; Zhou, Y.; et al. MDM2 is a useful prognostic biomarker for resectable gastric cancer. *Cancer Sci.* 2013, 104, 590-598.

17. Chen, X.; Feng, J.; Ge, Z.; Chen, H.; Ding, W.; Zhu, W.; Tang, X.; Chen, Y.; Tan, Y.; Ma, T. Effects of the JWA gene in the regulation of human breast cancer cells. *Mol. Med. Rep.* 2015, 11, 3848-3853.

18. Wu, Y.Y.; Ma, T.L.; Ge, Z.J.; Lin, J.; Ding, W.L.; Feng, J.K.; Zhou, S.J.; Chen, G.C.; Tan, Y.F.; Cui, G.X. JWA gene regulates PANC-1 pancreatic cancer cell behaviors through MEK-ERK1/2 of the MAPK signaling pathway. *Oncol. Lett.* 2014, 8, 1859-1863.

19. Lin, J.; Ma, T.; Jiang, X.; Ge, Z.; Ding, W.; Wu, Y.; Jiang, G.; Feng, J.; Cui, G.; Tan, Y. JWA regulates human esophageal squamous cell carcinoma and human esophageal cells through different mitogen-activated protein kinase signaling pathways. *Exp. Ther. Med.* 2014, 7, 1767-1771.

20. Li, Y.; Shen, X.; Wang, X.; Li, A.; Wang, P.; Jiang, P.; Zhou, J.; Feng, Q. EGCG regulates the cross-talk between JWA and topoisomerase IIα in non-small cell lung cancer (NSCLC) cells. *Sci. Rep.* 2015, 5, 11009.

21. Wang, Q.; Chen, Q.; Zhu, L.; Chen, M.; Xu, W.; Panday, S.; Wang, Z.; Li, A.; Røe, O.D.; Chen, R.; et al. JWA regulates TRAIL-induced apoptosis via MARCH8-mediated DR4 ubiquitination in cisplatin-resistant gastric cancer cells. *Oncogenesis.* 2017, 6, e353.

22. Liang, Y.; Qian, C.; Xie, Y.; Huang, X.; Chen, J.; Ren, Y.; Fu, Z.; Li, Y.; Zeng, T.; Yang, F.; et al. JWA suppresses proliferation in trastuzumab-resistant breast cancer by downregulating CDK12. *Cell Death Discovery.* 2021, 7, 306.

23. Li, X.; Liu, J.; Zhou, Y.; Wang, L.; Wen, Y.; Ding, K.; Zou, L.; Liu, X.; Li, A.; Wang, Y.; et al. Jwa participates the maintenance of intestinal epithelial homeostasis via ERK/FBXW7-mediated NOTCH1/PPARγ/STAT5 axis and acts as a novel putative aging related gene. *Int. J. Biol. Sci.* 2022, 18, 5503-5521.

24. Zhao, X.; Wang, R.; Xiong, J.; Yan, D.; Li, A.; Wang, S.; Xu, J.; Zhou, J. JWA antagonizes paraquat-induced neuro toxicity via activation of Nrf2. *Toxicol. Lett.* 2017, 277, 32-40.

25. Zhang, Y.; Chen, J.; Che, Z.; Shu, C.; Chen, D.; Ding, K.; Li, A.; Zhou, J. JP3 enhances the toxicity of cisplatin on drug-resistant gastric cancer cells while reducing the damage to normal cells. *J. Cancer.* 2021, 12, 1894-1906.

26. Zhou, Y.; Liu, J.; Li, X.; Wang, L.; Hu, L.; Li, A.; Zhou, J. JAC4 protects from X-ray radiation-induced intestinal injury by JWA-mediated anti-oxidation/inflammation signaling. *Antioxidants (Basel, Switzerland).* 2022, 11.

27. Zhou, J.; Ye, J.; Zhao, X.; Li, A.; Zhou, J. JWA is required for arsenic trioxide induced apoptosis in HeLa and MCF-7 cells via reactive oxygen species and mitochondria linked signal pathway. *Toxicol. Appl. Pharmacol*. 2008, 230, 33-40.

28. Hu, L.; Sun, F.; Sun, Z.; Ni, X.; Wang, J.; Wang, J.; Zhou, M.; Feng, Y.; Kong, Z.; Hua, Q.; et al. Apatinib enhances the radiosensitivity of the esophageal cancer cell line KYSE-150 by inducing apoptosis and cell cycle redistribution. *Oncol. Lett.* 2019, 17, 1609-1616.

29. Srinivas, U.S.; Tan, B.W.Q.; Vellayappan, B.A.; Jeyasekharan, A.D. ROS and the DNA damage response in cancer. *Redox Biol.* 2019, 25, 101084.

30. Miao, S.-H.; Sun, H.-B.; Ye, Y.; Yang, J.-J.; Shi, Y.-W.; Lu, M.; Hu, G.; Zhou, J.-W. Astrocytic JWA expression is essential to dopaminergic neuron survival in the pathogenesis of Parkinson's disease. *CNS Neurosci. Ther.* 2014, 20, 754-762.

31. Jain, V.; Berman, A.T. Radiation pneumonitis: old problem, New Tricks. *Cancers.* 2018, 10.

32. Xiong, L.; Tan, B.; Lei, X.; Zhang, B.; Li, W.; Liu, D.; Xia, T. SIRT6 through PI3K/Akt/mTOR signaling pathway to enhance radiosensitivity of non-small cell lung cancer and inhibit tumor progression. *IUBMB Life.* 2021, 73, 1092-1102.

33. Du, M.; Wang, J.; Chen, H.; Wang, S.; Chen, L.; Xu, Y.; Su, F.; Lu, X. MicroRNA-200a suppresses migration and invasion and enhances the radiosensitivity of NSCLC cells by inhibiting the HGF/c-Met signaling pathway. *Oncol. Rep.* 2019, 41, 1497-1508.

34. Xue, A.; Shang, Y.; Jiao, P.; Zhang, S.; Zhu, C.; He, X.; Feng, G.; Fan, S. Increased activation of cGAS-STING pathway enhances radiosensitivity of non-small cell lung cancer cells. *Thorac. Cancer.* 2022, 13, 1361-1368.

35. Lei, X.; Du, L.; Zhang, P.; Ma, N.; Liang, Y.; Han, Y.; Qu, B. Knockdown GTSE1 enhances radiosensitivity in non-small cell lung cancer through DNA damage repair pathway. *J. Cell. Mol. Med.* 2020, 24, 5162-5167.

36. Li, Y.; Sun, C.; Tan, Y.; Zhang, H.; Li, Y.; Zou, H. ITGB1 enhances the radioresistance of human non-small cell lung cancer cells by modulating the DNA damage response and YAP1-induced epithelial-mesenchymal transition. *Int. J. Biol. Sci.* 2021, 17, 635-650.

37. Raghavan, P.; Tumati, V.; Yu, L.; Chan, N.; Tomimatsu, N.; Burma, S.; Bristow, R.G.; Saha, D. AZD5438, an inhibitor of cdk1, 2, and 9, enhances the radiosensitivity of non-small cell lung carcinoma cells. *Int. J. Radiat. Oncol. Biol. Phys.* 2012, 84, e507-e514.

38. Wu, Z.; Qiu, M.; Guo, Y.; Zhao, J.; Liu, Z.; Wang, H.; Meng, M.; Yuan, Z.; Mi, Z. OTU deubiquitinase 4 is silenced and radiosensitizes non-small cell lung cancer cells via inhibiting DNA repair. *Cancer. Cell. Int.* 2019, 19, 99.

39. Blackford, A.N.; Jackson, S.P. ATM, ATR, and DNA-PK: the trinity at the heart of the DNA damage response. *Mol. Cell.* 2017, 66, 801-817.

40. Jette, N.; Lees-Miller, S.P. The DNA-dependent protein kinase: a multifunctional protein kinase with roles in DNA double strand break repair and mitosis. *Prog. Biophys. Mol. Biol.* 2015, 117, 194-205.

41. Liu, Y.; Gao, F.; Jiang, H.; Niu, L.; Bi, Y.; Young, C.Y.F.; Yuan, H.; Lou, H. Induction of DNA damage and ATF3 by retigeric acid B, a novel topoisomerase II inhibitor, promotes apoptosis in prostate cancer cells. *Cancer Lett.* 2013, 337, 66-76.

42. Borgstahl, G.E.O.; Oberley-Deegan, R.E. Superoxide Dismutases (SODs) and SOD mimetics. *Antioxidants (Basel, Switzerland).* 2018, 7.

43. Glorieux, C.; Zamocky, M.; Sandoval, J.M.; Verrax, J.; Calderon, P.B. Regulation of catalase expression in healthy and cancerous cells. *Free Radic. Biol. Med.* 2015, 87, 84-97.

44. Gaweł, S.; Wardas, M.; Niedworok, E.; Wardas, P. Malondialdehyde (MDA) as a lipid peroxidation marker. *Wiadomosci Lekarskie (Warsaw, Poland: 1960).* 2004, 57, 453-455.

45. Ahmadvand, M.H.; Nikzad, S.; Changizi, V.; Pashaki, A.S.; Najafi, M.; Mirzaei, F. Evaluation of the mitigation effect of spirulina against lung injury induced by radiation in rats. *Current Radiopharm.* 2022.

46. Du, Y.; Jia, C.; Liu, Y.; Li, Y.; Wang, J.; Sun, K. Isorhamnetin enhances the radiosensitivity of A549 cells through interleukin-13 and the NF-κB signaling pathway. *Front. Pharmacol.* 2020, 11, 610772.

47. Arroyo-Hernández, M.; Maldonado, F.; Lozano-Ruiz, F.; Muñoz-Montaño, W.; Nuñez-Baez, M.; Arrieta, O. Radiation-induced lung injury: current evidence. *BMC Pulm. Med.* 2021, 21, 9.

48. Rodrigues, G.; Lock, M.; D'Souza, D.; Yu, E.; Van Dyk, J. Prediction of radiation pneumonitis by dose-volume histogram parameters in lung cancer--a systematic review. *Radiother. Oncol.* 2004, 71, 127-138.

49. Yang, M.; Fan, Q.; Hei, T.K.; Chen, G.; Cao, W.; Meng, G.; Han, W. Single-cell transcriptome analysis of radiation pneumonitis mice. *Antioxidants (Basel, Switzerland).* 2022, 11.

 doi:10.20944/preprints202306.0356.v1

50. Decout, A.; Katz, J.D.; Venkatraman, S.; Ablasser, A. The cGAS-STING pathway as a therapeutic target in inflammatory diseases. *Nat. Rev. Immunol.* 2021, 21, 548-569.